Chapter 5

Time sequences for pulsed magnetic focusing

"There is a time for everything, and a season for every activity under heaven." Ecclesiastes 3v1

This chapter will describe how the timing sequences are calculated for the magnetic lens pulses. The experimental model described in Section 3.2 is still used to give quantitative results. Initially the laser guide is not used, and magnetic lenses are used to refocus the ballistically expanded cloud. In simulating the lens performance, a maximum of $NI = 10,000$ Amps in the current coils were used. Work contained within this chapter led to the publication of refs. [141, 145, 146] and has been done in collaboration with the other authors.

5.1 $\mathcal{ABCD}$ matrices

The harmonic accelerations in eqn. (4.3) and eqn. (4.4) lead to three separable one-dimensional simple harmonic oscillator equations for the atomic motion. It is useful to employ the $\mathcal{ABCD}$-matrix formulation used widely in geometrical optics. The initial (subscript i) and final position and velocity of an atom along

a given Cartesian axis, say x, are related via the equation:

$$\begin{pmatrix} x \\ v_x \end{pmatrix} = \begin{pmatrix} \mathcal{A} & \mathcal{B} \\ \mathcal{C} & \mathcal{D} \end{pmatrix} \begin{pmatrix} x_{\mathrm{i}} \\ v_{x_{\mathrm{i}}} \end{pmatrix}. \tag{5.1}$$

To simplify the effects of gravity, the calculations are performed in a free-falling frame of reference. In this frame the free evolution of the cloud is an isotropic expansion, described by an $\mathcal{ABCD}$ matrix. The influence of a converging or diverging magnetic lens can also be described by $\mathcal{ABCD}$ matrices, as outlined in [52, 156]:

$$M_1(t) = \begin{pmatrix} 1 & t \\ 0 & 1 \end{pmatrix}, \tag{5.2}$$

$$M_2(\omega, \tau) = \begin{pmatrix} \cos\omega\tau & \frac{1}{\omega}\sin\omega\tau \\ -\omega\sin\omega\tau & \cos\omega\tau \end{pmatrix}, \tag{5.3}$$

$$M_3(\omega, \tau) = \begin{pmatrix} \cosh\omega\tau & \frac{1}{\omega}\sinh\omega\tau \\ \omega\sinh\omega\tau & \cosh\omega\tau \end{pmatrix}. \tag{5.4}$$

Matrix M_1 is the translation matrix for a duration t; M_2 is the matrix for a converging lens of strength ω applied for a duration τ; M_3 is the matrix for a diverging lens of strength ω applied for a duration τ. It is interesting to note that the sinusoidal (exponential) path taken by atoms inside a converging (diverging) magnetic lens is in stark contrast to the linear propagation of light rays in an optical lens.

By multiplying these matrices together, one arrives at the final $\mathcal{ABCD}$ system matrix. An image (i.e. a one-to-one map of position between the initial and final cloud) is formed if the condition $\mathcal{B} = 0$ is maintained. In this case the spatial magnification $\mathcal{A}$ is the inverse of the velocity magnification $\mathcal{D}$. This spatial compression and concomitant velocity spread is a manifestation of Liouville's theorem (see for example ref. [144]). The theorem states that phase-space density is conserved in a Hamiltonian system. Time-dependent Stern-Gerlach forces satisfy the criteria for Liouville's theorem to be valid [157]. The cloud extent along x in a given plane is given by:

$${\sigma_x}^2 = (\mathcal{A}\sigma_{x_i})^2 + (\mathcal{B}\sigma_{v_{x_i}})^2, \tag{5.5}$$

where σ_{x_i} is the initial position standard deviation and $\sigma_{v_{x_i}}$ is the initial velocity standard deviation. An *image* is formed for the condition $\mathcal{B} = 0$, but the *smallest cloud size* occurs when one minimises the product of the cloud extent for all 3 spatial dimensions (i.e. $\sigma_x\sigma_y\sigma_z$). For single- and double-impulse lens systems modelled using the full magnetic field expressions, the cloud size at the image plane and the minimum cloud size do not correspond exactly, but they are usually very similar. The rest of this thesis will consider the cloud size at the image plane ($\mathcal{B} = 0$), and thus $\mathcal{A}$ corresponds to the magnification.

5.1.1 Thick and thin lenses

The finite pulse time means the atom's position and velocity will be modified during the pulse and therefore the simple focusing formulae of 'thin lens' optics cannot be used. A mathematical transformation can be made from the lab frame of 'thick lenses' to 'thin lenses'. A thick converging lens M_2 is identical to a thin lens of strength $\mathcal{C}(\omega,\tau) = -\omega\sin(\omega\tau)$ (i.e. the original $\mathcal{C}$ entry of the M_2 $\mathcal{ABCD}$ matrix), pre- and post-multiplied by a translation matrix with duration $\tau'/2$:

$$M_2 = \begin{pmatrix} 1 & \tau'/2 \\ 0 & 1 \end{pmatrix} \begin{pmatrix} 1 & 0 \\ \mathcal{C} & 1 \end{pmatrix} \begin{pmatrix} 1 & \tau'/2 \\ 0 & 1 \end{pmatrix}. \tag{5.6}$$

The effective pulse width τ' is defined as:

$$\tau'(\omega,\tau) = \frac{2}{\omega}\tan\frac{\omega\tau}{2}, \tag{5.7}$$

and the notation of primes is used to denote times in the thin lens representation. This means many of the simplicities of thin lens optics can be used, even when dealing with the more accurate thick lensing behavior. The effective thin lens duration of the pulse τ' differs from the actual pulse duration τ, but otherwise the treatments are identical. In the limit of a short, strong pulse $\omega\tau \to 0$, one finds that $\tau' \to \tau$. If one wishes to consider the diverging lens M_3, merely make the transformation $\omega \to i\omega$ in eqn. (5.6) – i.e. $\mathcal{C} = \omega\sinh(\omega\tau)$ and $\tau' = \frac{2}{\omega}\tanh\frac{\omega\tau}{2}$.

5.2 Single-impulse focusing

A single lens system can be modelled by having a translation of $M_1(t_1')$, where $t_1' = t_1 + \tau'/2$, followed by a thin lens of strength $\mathcal{C}$, followed by a translation of $M_1(t_2')$, where $t_2' = t_2 + \tau'/2$. The $\mathcal{ABCD}$ matrix sequence is:

$$\begin{pmatrix} \mathcal{A} & \mathcal{B} \\ \mathcal{C} & \mathcal{D} \end{pmatrix} = \begin{pmatrix} 1 & t_2' \\ 0 & 1 \end{pmatrix} \begin{pmatrix} 1 & 0 \\ \mathcal{C} & 1 \end{pmatrix} \begin{pmatrix} 1 & t_1' \\ 0 & 1 \end{pmatrix}, \tag{5.8}$$

The physical duration of the focusing is $T = t_1 + t_2 + \tau$, however the thin lens system has a total time $T' = t_1 + t_2 + \tau' = T - \tau + \tau'$, see Figure 5.1.

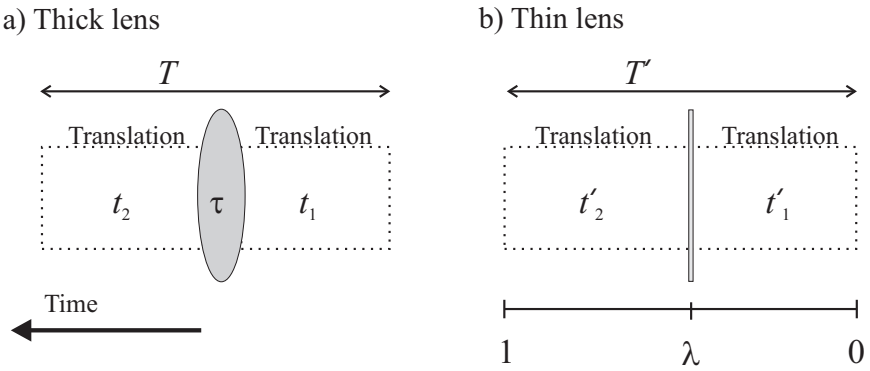

Figure 5.1: A diagram showing the single-impulse timing sequence for the two frames of reference: (a) shows the thick lens or lab frame with the time durations for each stage and (b) shows the mathematically equivalent thin lens representation that is used in the calculations. Note that the direction of time runs right to left so that it visually mirrors the system matrix layout in eqn. (5.8). The dimensionless timing parameter λ is also shown in (b).

For a single lens system, the condition $\mathcal{B} = 0$ is met for the system $\mathcal{ABCD}$ matrix if:

$$\mathcal{C}T' = \frac{1}{\lambda(\lambda - 1)}, \tag{5.9}$$

where a dimensionless parameter to represent the timing of the lens pulse has been defined[1]:

$$\lambda = \frac{t_1'}{T'}. \tag{5.10}$$

This formalism provides a useful way of designing a lens system and investigating its focusing properties.

[1]In hindsight the use of λ is confusing when dealing with wavelengths, however to be consistent with previous work the notation is continued.

The magnification of such a system is given by:

$$M_{\rm ag} = \frac{(\lambda - 1)}{\lambda}. \tag{5.11}$$

The density increase from a single-impulse isotropic 3D harmonic lens is given by: $-{M_{\rm ag}}^{-3} = \lambda^3/(1-\lambda)^3$. For a converging lens, eqn. (5.9) becomes:

$$\omega T' \sin \omega\tau = \frac{1}{\lambda(1-\lambda)}. \tag{5.12}$$

Considering an experimental situation where the total time ($T = 212\,\mathrm{ms}$) and the maximum coil current ($NI = 10,000$ Amps) are fixed. The geometry of the lens then fixes the maximum strength of the lens. For the specific case of a 4 cm radius Strategy I lens (radial curvature $\omega_r = 98.4\,\mathrm{rad\,s^{-1}}$ from eqn. (4.16)) the analytic result for $\lambda(\omega, \tau)$ is illustrated in Figure 5.2.

The $\lambda(\omega, \tau)$ parameter is maximised (and the magnification $M_{\rm ag}$ is minimised) when:

$$1 - \omega(T - \tau)\cot \omega\tau = 0, \tag{5.13}$$

which has the solution $\lambda = 0.95$ at $\tau = 15.4\,\mathrm{ms}$. This corresponds to a reduction in the radial atomic cloud size by a factor of 19. This is achieved when the pulse duration τ is from time $t = T - \tau$ to $t = T$, i.e. the lens pulse ends at the time of focus. Such focusing in three dimensions would increase the cloud density by more than 3 orders of magnitude. For a lens placed later in time, the magnetic pulse would not have finished at the predicted focal time T, resulting in an increase in cloud size at time T.

The above analysis would seem to suggest that the optimum strategy for achieving the smallest cloud size would be to construct a lens with a short, strong pulse $\omega\tau \to 0$, and use the latest possible pulse time $\lambda \to 1$. However, experimental constraints and lens aberrations alter the above conclusion.

5.2.1 Lenses with a constant $\mathbf{a}_0$ term

In Chaper 4 Strategy IV and V lenses had a constant acceleration, $\mathbf{a}_0$, due to the axial asymmetry. For realistic lens parameters the constant acceleration's magnitude is on the order of 100 m s^{-2} (eqn. (4.19)). Typically the acceleration

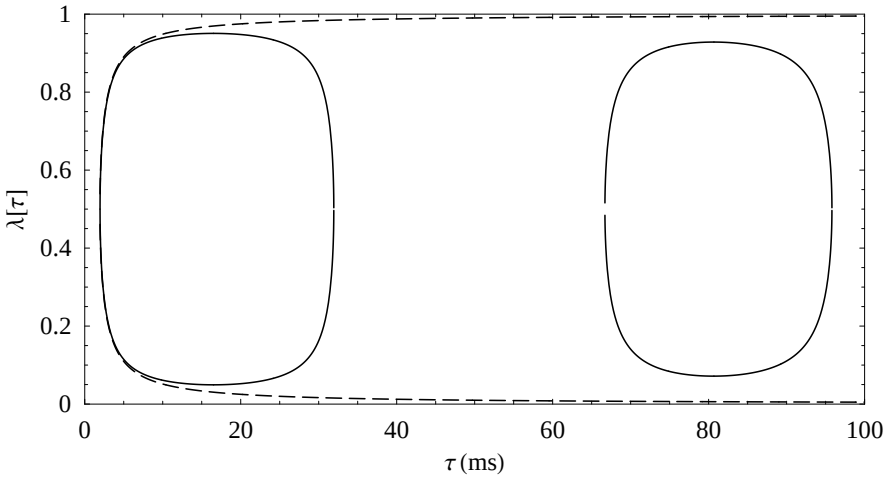

Figure 5.2: By fixing the strength of a Strategy I radially converging lens, $\omega_r = 98.4\ \mathrm{rad\,s^{-1}}$, and total experimental focusing time $T = 212\,\mathrm{ms}$, one can vary the lens pulse width, τ, and find the focusing parameter $\lambda(\tau)$ via eqn. (5.12). The impulse τ has a minimum of 2.0 ms at $\lambda = 0.5$, and λ is symmetric about this point. Also shown (dashed) is the result obtained if one makes the strong, short pulse approximation $\omega\tau \to 0$, leading to the simplification $\sin\omega\tau \approx \omega\tau$ in eqn. (5.12) - resulting unsurprisingly in a divergence for large pulse durations.

changes the cloud's vertical velocity by about 1 m s^{-1}. Depending on the lens' orientation this can either slow or accelerate the atomic cloud's flight, see Figure 5.3. The initial launch velocity has to be modified to take this change into account so that the cloud apex remains at the required height. As an aside, it should be noted that the ability to accelerate or decelerate a cloud could have uses in a horizontal transport scheme as a means to modify the centre of mass motion.

Based upon a simple trajectory model that incorporates three stages of acceleration ($-g$ when $\{0 < t < t_1\}$ and $\{t_1 + \tau < t < T\}$; $\mathbf{a}_0 - g$ when $\{t_1 < t < t_1 + \tau\}$), and ensuring that the centre of mass comes to rest at a height h, the required launch velocity is:

$$v_{z_i} = \mathbf{a}_0\tau + \sqrt{g(2h + \mathbf{a}_0(t_1 + \tau)(t_1 - \tau))}\,, \tag{5.14}$$

and the apex time of such a flight path is:

$$T = \frac{v_{z_i} - \mathbf{a}_0\tau}{g}\,. \tag{5.15}$$

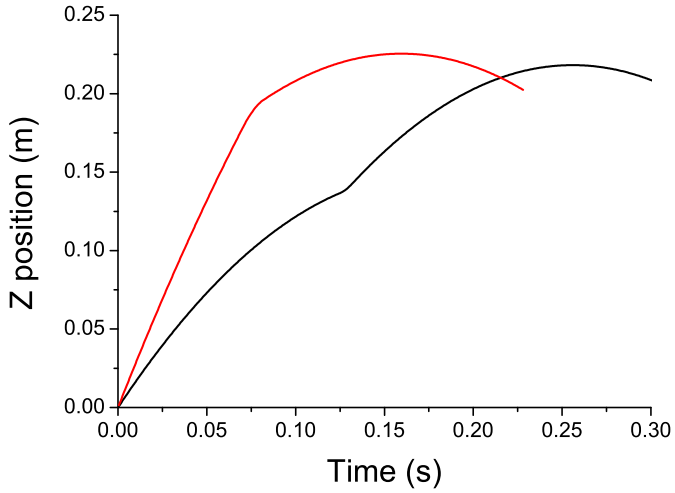

Figure 5.3: The atomic cloud centre of mass' vertical position is plotted against time for a decelerating (red line) and an accelerating (black line) axial-only lens (Strategy IV). The magnetic pulse occurs at $\lambda = 0.5$ and the initial velocity was set so that the apex occurs at $h = 0.22$ m. The decelerating (accelerating) lens requires a faster (slower) launch velocity and the flight time is shorter (longer).

As expected when $\mathbf{a}_0 = 0$ these return to the free-flight launch velocity $v_{z_i} = \sqrt{2gh}$ and apex time $T = \sqrt{2h/g}$. Ensuring that the focus occurs at the same time as the cloud's apex is non-trivial. The pulse length is calculated based upon knowledge of the required focus time, see eqn. (5.12). But the focus time depends upon the location, duration and strength of the magnetic pulse. Solving the problem requires iteration.

A further complication arises in the case of a decelerating lens due to the fact that the vertical launch velocity, v_{z_i}, can become complex for some t_1 and τ values. The physical situation that corresponds to this case is where the desired apex height has been reached before the pulse has finished. One finds that this limits the maximum λ that can be used. The situation is worse for larger radius lenses as these require longer pulse durations to achieve focusing. The accelerating lens does not suffer from this kind of upper bound on λ.

5.3 Double-impulse focusing

A double lens system, see Figure 5.4, comprising of lenses of strength and duration ω_1, τ_1 (starting after a time t_1) and ω_2, τ_2 (starting a time t_2 after the first lens) is modelled by using the following $\mathcal{ABCD}$ matrix sequence:

$$\begin{pmatrix} \mathcal{A} & \mathcal{B} \\ \mathcal{C} & \mathcal{D} \end{pmatrix} = \begin{pmatrix} 1 & t_3' \\ 0 & 1 \end{pmatrix} \begin{pmatrix} 1 & 0 \\ \mathcal{C}_2 & 1 \end{pmatrix} \begin{pmatrix} 1 & t_2' \\ 0 & 1 \end{pmatrix} \begin{pmatrix} 1 & 0 \\ \mathcal{C}_1 & 1 \end{pmatrix} \begin{pmatrix} 1 & t_1' \\ 0 & 1 \end{pmatrix}, \quad (5.16)$$

i.e. a $t_1' = t_1 + \frac{1}{2}\tau_1'$ translation, then a strength $\mathcal{C}_1$ thin lens, a $t_2' = \frac{1}{2}\tau_1' + t_2 + \frac{1}{2}\tau_2'$ translation, then a strength $\mathcal{C}_2$ thin lens followed by a $t_3' = T' - t_1' - t_2'$ translation, where $\mathcal{C}_j = -\omega_j \sin(\omega_j \tau_j)$ and $\tau_j' = \frac{2}{\omega_j} \tan(\frac{\omega_j \tau_j}{2})$ for $j \in \{1, 2\}$. The total physical duration of the focusing, T, is fixed, and the effective total time of the double lens system is $T' = T - \tau_1 - \tau_2 + \tau_1' + \tau_2'$.

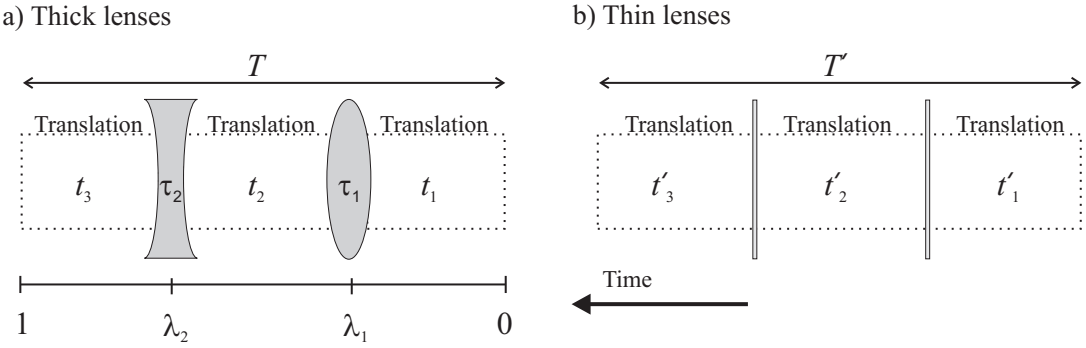

Figure 5.4: A diagram showing the double-impulse timing sequence for the two frames of reference: (a) shows the thick lens or lab frame with the time durations for each stage and (b) shows the mathematically equivalent thin lens representation that is used in the calculations. Note that the direction of time runs right to left so that it visually mirrors the system matrix layout in eqn. (5.16). The dimensionless timing parameters λ_1 and λ_2 are also shown in (a).

The important entries of the system matrix in eqn. (5.16) are $\mathcal{A}$ and $\mathcal{B}$:

$$\mathcal{A} = 1 + (\mathcal{C}_1 + \mathcal{C}_2)(T' - t_1') + \mathcal{C}_2(-1 + \mathcal{C}_1(T' - t_1'))t_2' - \mathcal{C}_1\mathcal{C}_2 {t_2'}^2, \quad (5.17)$$

$$\mathcal{B} = T' + \mathcal{C}_2(T' - t_1' - t_2')(t_1' + t_2') + \mathcal{C}_1 t_1'(T' + \mathcal{C}_2(T' - t_2')t_2' - t_1'(1 + \mathcal{C}_2 t_2')), \quad (5.18)$$

which are both second order in t_1' and t_2' (and hence also second order in t_1 and t_2).

To obtain an atom cloud which is focused in all 3 dimensions requires that the first lens is axially converging (radially diverging) and the second lens is axially diverging (radially converging), or vice versa. Moreover, the radial (subscript r) and axial (subscript z) spatial dimensions have different $\mathcal{A}$ and $\mathcal{B}$ coefficients. If the two axial lens strengths are ω_{1z} and ω_{2z}, then eqn. (4.17) yields $\omega_{1r} = \mathrm{i}\omega_{1z}/\sqrt{2}$ and $\omega_{2r} = \mathrm{i}\omega_{2z}/\sqrt{2}$. A 3D image is formed when eqn. (5.18) is set equal to zero for both the radial and axial directions.

In Section 5.2 the density increase from a single-impulse isotropic 3D harmonic lens, $\lambda^3/(1-\lambda)^3$, could be characterised by λ, the equivalent time of the thin lens, $t_1{}'$, relative to the total equivalent focus time T'. Note that for the anisotropic lenses in this section the *equivalent* (i.e. thin lens) timing of a lens in the radial and axial direction is different.

For this reason alternate-gradient lensing is characterised with the parameters:

$$\{\lambda_1, \lambda_2\} = \left\{ \frac{t_1 + \tau_1/2}{T}, \frac{t_1 + \tau_1 + t_2 + \tau_2/2}{T} \right\}, \tag{5.19}$$

corresponding to the mean times of the first and second magnetic impulses relative to the total experimental lensing time T. This labelling is used if ω_{1r} is real (the first lens is radially converging), and the definitions in eqn. (5.19) are swapped if ω_{1r} is imaginary (the first lens is radially diverging). Therefore λ_1 (λ_2) represents the timing of the radially (axially) converging lens.

As before, the coils are assumed to have a 4 cm radius with $NI = 10,000$ Amps in each coil. The two lens combinations in Figure 4.7 are shown in the table below with the resulting angular frequencies.

Strategy	1st lens	ω_{1r}	S_1	2nd lens	ω_{2r}	S_2	ξ
AR	Axial focus	$58\mathrm{i}\,\mathrm{rad\ s^{-1}}$	2.63	Radial focus	$98\,\mathrm{rad\ s^{-1}}$	0.58	> 1
RA	Radial focus	$98\,\mathrm{rad\ s^{-1}}$	0.58	Axial focus	$58\mathrm{i}\,\mathrm{rad\ s^{-1}}$	2.63	< 1

Table 5.1: The two different alternate-gradient strategies modelled. The ω's are the lens strengths of the 4 cm radii coils, S's are the coil separations and $\xi = \sigma_z/\sigma_r$ is the cloud aspect ratio.

For a range of values of τ_1, and τ_2, the radial and axial simultaneous eqns. (5.18) (i.e. $\mathcal{B}_r = 0$, $\mathcal{B}_z = 0$) are solved to determine t_1 and t_2. Although both $\mathcal{B}_z$ and $\mathcal{B}_r$ are quadratic in t_1 and t_2, substitution for either of these variables leads to a final sextic polynomial equation. This must therefore be solved numerically and leads

to six solution pairs (t_1, t_2). Only solution pairs with real times $0 \leq t_1, t_2 \leq T$ satisfying the condition $t_1 + \tau_1 + t_2 + \tau_2 \leq T$ are considered. The number of (t_1, t_2) solution pairs as a function of τ_1 and τ_2 is shown in Figure 5.5 (a). These (t_1, t_2) solution pairs can then be used to calculate the relative increase in atomic density of a cold atom cloud. From eqn. (5.5) the relative density increase of the image is thus:

$$\rho_{3D} = \frac{{\sigma_R}^3}{((\mathcal{A}_r\sigma_R)^2 + (\mathcal{B}_r\sigma_V)^2)\sqrt{(\mathcal{A}_z\sigma_R)^2 + (\mathcal{B}_z\sigma_V)^2}} \rightarrow \frac{1}{{\mathcal{A}_r}^2\mathcal{A}_z}, \tag{5.20}$$

where σ_R and σ_V are 1D standard deviations of the isotropic cold atom cloud's initial spatial and velocity distributions, and the arrow indicates the limit $\mathcal{B} = 0$. The dimensionless relative density increases obtained for both strategies are shown in Figures 5.5 (b) and (c). These plots are then effectively combined in Figure 5.5 (d) by inverting τ_1, τ_2 to find the relative density increase as a function of the parameters λ_1, λ_2 which are the mean relative times of the radially converging and diverging lens.

Chapter 5 summary

- The $\mathcal{ABCD}$ formalism was introduced to describe lens systems.
- A transformation was used to convert 'thick' parabolic lenses into mathematically equivalent 'thin' lenses.
- An equation to obtain the required pulse length for single-impulse focusing was presented. This was then used to show that there exists a theoretical limit on how small a focus that can be produced.
- A simple model to account for lenses that have a constant acceleration term was explained.
- The method to obtain the correct pulse sequence for focusing using the alternate-gradient scheme was outlined.

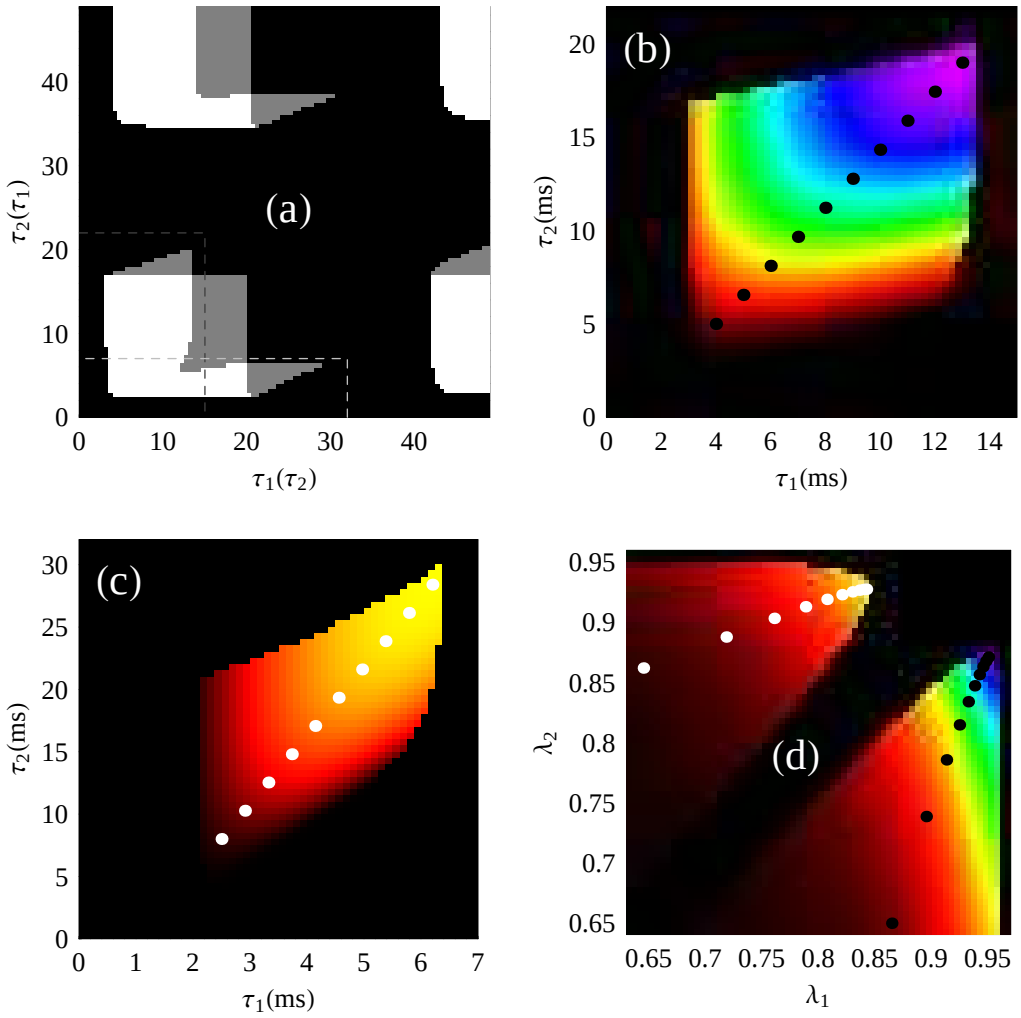

Figure 5.5: Image (a) shows the number of solution pairs (black=0, grey=1, white=2) for (t_1, t_2) as a function of τ_1 and τ_2 (τ_2 and τ_1) in ms for Strategy AR (Strategy RA). The two dashed regions of the 'solution island' lead to the highest relative density increases, shown in (b) for Strategy AR and (c) for Strategy RA. The relative density increase (eqn. (5.20)) if one images a cloud of atoms using: (b) Strategy AR, (c) Strategy RA. The maximum relative density increases are 1100 (320), for a $\xi = \sigma_z/\sigma_r = 17$ sausage ($\xi = 0.094$ pancake) shaped cloud, for images (b) and (c) respectively. The results of (b) and (c) are combined in (d), the relative density increase in terms of λ_1 and λ_2 (the mean times of the radially converging and radially diverging impulses relative to T). The points in images (b)-(d) are used in the next chapter as a sample in simulations. [Figure generated in collaboration with A. S. Arnold.]